Prediction of Payload Vibration Environments by Mechanical Admittance Test Techniques

Daniel D. Kana* and Luis M. Vargas†
Southwest Research Institute, San Antonio, Texas

A series of experiments were conducted with simple beam and mass launch vehicle and payload models in order to determine the validity of mechanical admittance/impedance techniques applied to development of improved payload vibration tests. Admittance and impedances were measured from tests of the individual components to form matrices which were combined analytically to allow prediction of responses for the complete system. Results were computed for a transmission matrix approach and an admittance matrix approach. Only results for the admittance method appeared to be satisfactory when compared to measurements on the combined system.

Introduction

PRESENT plans call for frequent missions to be flown by the space shuttle to ferry a variety of payloads to and from earth orbit. Each payload is likely to have different dynamic characteristics, and may couple significantly with responses of the orbiter vehicle. Thus, each payload must be qualified to its own tailored anticipated vibration environment, in spite of the fact that all payloads will be flown in the same or similar orbiter vehicles. Furthermore, cost effectiveness requires testing the payload alone, although dynamic interaction with the orbiter must be accounted for at the attach points.

It is apparent that simplicity must be a very necessary ingredient of improved payload vibration test procedures if a reasonably economical approach is to be developed. Nevertheless, the essential difference of each test to be performed cannot be overlooked. Therefore, the application of mechanical admittance/impedance concepts in the development of test specifications has been considered as a possible means of achieving some measure of simplicity. That is, characteristics of the orbiter alone will not change from flight to flight, although those of the payloads will. Therefore, if appropriate admittances for the payload and orbiter are determined from tests of each component individually, the results can be combined analytically to allow prediction of the payload environments for various flight operations. Therefore, only one test series need be run for the orbiter, although each payload must be investigated individually. Nevertheless, the combined environment can be predicted for all payload/orbiter combinations.

The application of admittance techniques to the problem at hand appears to be relatively straightforward. However, from previous experience it is known that admittance/impedance parameters vary over several orders of magnitude in complex structures, and measurement errors can have a significant influence on results predicted for the combined system. Therefore, the purpose of the program described herein has been to test the validity of this approach on a relatively simple orbiter/payload model. Physical models were built so that admittance tests could be run individually. Sufficient data were measured to form frequency-dependent matrix representations of the component characteristics. These matrices were combined analytically to allow prediction of payload model responses to subsequent orbiter model excitation for the coupled system. Further, tests were then conducted on the combined physical models to provide data for correlation with the predictions.

Thus, the present study includes tests on conceptual physical models which bear little resemblance to an actual space shuttle orbiter or payload. For purposes of analogy, however, hereafter the terminology "orbiter" or "payload" will be used to describe these simple models. Furthermore, it should be recognized that, although the impetus for this study arose from space shuttle considerations, the methods studied are, of course, applicable to launch vehicles in general. Consequently, the results expand upon earlier work reported by Klosterman,[1] Berman and Flannelly,[2] and others.

From the onset of this program, it was recognized that several sources of measurement error could influence the final results, and also as the program progressed, it became apparent that slight alterations in the approach could yield more useful information. Thus, two somewhat different analytical methods (transmission matrix and admittance matrix) will be described, although it will be shown that only one provided useful results for this application.

Analytical Models

The desired objective is to predict the response of a payload when external excitation is applied to the orbiter. For this, the required method is to utilize mechanical admittance or related response parameter concepts, when the parameters have been determined by experiment. It is recognized that several approaches to this problem are possible, depending on whether impedance, admittance, or transmission matrix methods are used. Initially, a transmission matrix approach will be presented, and then a simpler direct admittance approach will follow.

Transmission Matrix Formulation

General Equations

This development will follow that originally presented by Rubin,[3] although the notation is somewhat different. The proposed model orbiter/payload combination is shown in state space in Fig. 1. First consider the payload as a separate component and write its response in terms of an admittance matrix as

$$\begin{Bmatrix} A_2 \\ A_2' \end{Bmatrix} = \begin{bmatrix} E_2 & G_2{}^T \\ G_2 & H_2 \end{bmatrix} \begin{Bmatrix} -F_2 \\ F_2' \end{Bmatrix} \tag{1}$$

where E_2, G_2, and H_2 are submatrices having complex elements, and are formed by partitioning the bracketed complete admittance matrix; A_2, F_2 are acceleration and force vectors, respectively. Note that primed quantities represent the input variables and unprimed quantities the output variables. Also, the subscript 2 refers to the payload, while

Presented as Paper 75-812 at the AIAA/ASME/SAE 16th Structures, Structural Dynamics, and Materials Conference, Denver, Colorado, May 27-29, 1975; received May 28, 1975; revision received August 14, 1975. The authors wish to express their sincere appreciation to several individuals who contributed to this program. P.A. Cox aided with the transmission matrix formulation; H.Pennick and R.L. Bessey provided aid with computer programming. Experiments were conducted by G. Downey and M. Wood. Finally, numerous suggestions were provided by B.R. Hanks and R.W. Fralich of NASA Langley Research Center. This research was supported by NASA Langley Research Center under contract.

Index category: Structural Dynamic Analysis.

*Section Manager.

†Engineer.

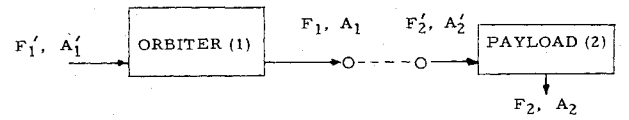

Fig. 1 Conceptual orbiter/payload system. F_1' ~excitation forces to orbiter; assumed known. A_1' ~excitation accelerations to orbiter; assumed known. F_1 ~output forces on orbiter at payload attach points; unknown. A_1 ~output accelerations on orbiter at payload attach points; unknown. F_2' ~input forces to payload at orbiter attach points; unknown. A_2' ~input accelerations to payload at orbiter attach points; unknown. F_2 ~response forces at payload; for free response, $F_2=0$. A_2 ~response accelerations of payload; unknown.

subscript 1 refers to the orbiter. By normal convention, positive forces are those applied *to* the terminals in admittance matrix formulations; however, for a transmission matrix, positive forces are applied to the input and *by* the output. Since a transmission matrix will be derived from the above admittance matrix, a negative sign has been added to the output force vector F_2. Thus, in forming the admittance matrix from experimental data, the forces applied *to* the structure can all be treated as positive, and the negative sign introduced in Eq. (1) will provide the correct sign to elements in the transmission matrix to follow.

$$A_2=-E_2F_2+G_2{}^TF_2' \tag{2}$$

$$A_2'=-G_2F_2+H_2F_2' \tag{3}$$

Premultiply Eq. (3) by G_2^T to obtain

$$G_2^TA_2'=-G_2^TG_2F_2+G_2^TH_2F_2'$$

Note that $G_2^TG_2$ is a square matrix and has an inverse, providing that there are not more outputs than inputs (i.e., G_2 is not a wide matrix). Therefore

$$(G_2^TG_2)^{-1}G_2^TA_2'=-F_2+(G_2^TG_2)^{-1}G_2^TH_2F_2' \tag{4}$$

If the left inverse of G_2 is labeled as

$$g_{2\ell}=(G_2^TG_2)^{-1}G_2^T$$

then from Eq. (4) there results

$$F_2=g_{2\ell}H_2F_2'-g_{2\ell}A_2' \tag{5}$$

Substituting Eq. (5) into Eq. (2),

$$A_2=(-E_2g_{2\ell}H_2+G_2^T)F_2'+E_2g_{2\ell}A_2' \tag{6}$$

If the number of response points on the payload is less than the number of attach points, then a rearward transmission matrix can be written from Eqs. (5) and (6) as

$$\begin{Bmatrix} F_2 \\ A_2 \end{Bmatrix}=\begin{bmatrix} J_2 & B_2 \\ C_2 & D_2 \end{bmatrix}\begin{Bmatrix} F_2' \\ A_2' \end{Bmatrix} \tag{7}$$

where

$$J_2=g_{2\ell}H_2, \quad B_2=-g_{2\ell}, \tag{8a), (8b)}$$

$$C_2=-E_2g_{2\ell}H_2+G_2^T, \quad D_2=E_2g_{2\ell} \tag{8c), (8d)}$$

and recall $g_{2\ell}=(G_2^TG_2)^{-1}G_2^T$. The restrictions on numbers of response and attach points result from maximum use of information available. For further details, see Reference 3.

Now similarly consider an admittance matrix for the orbiter

$$\begin{Bmatrix} A_1 \\ A_1' \end{Bmatrix}=\begin{bmatrix} E_1 & G_1{}^T \\ G_1 & H_1 \end{bmatrix}\begin{Bmatrix} -F_1 \\ F_1' \end{Bmatrix} \tag{9}$$

The same steps utilized for the payload yield a rearward transmission matrix for the orbiter

$$\begin{Bmatrix} F_1 \\ A_1 \end{Bmatrix}=\begin{bmatrix} J_1 & B_1 \\ C_1 & D_1 \end{bmatrix}\begin{Bmatrix} F_1' \\ A_1' \end{Bmatrix} \tag{10}$$

where

$$J_1=g_{1\ell}H_1 \tag{11a}$$

$$B_1=-g_{1\ell} \tag{11b}$$

$$C_1=-E_1g_{1\ell}H_1+G_1^T \tag{11c}$$

$$D_1=E_1g_{1\ell} \tag{11d}$$

and

$$g_{1\ell}=(G_1^TG_1)^{-1}G_1^T \tag{11e}$$

These results can now be combined to predict response for the orbiter/payload combination. For linear structures in series, the combined response can be obtained by the proper combination of the transmission matrices. For rearward transmission matrices

$$\psi=T_qT_{q-1}\ldots T_2T_1\psi'$$

where ψ is the state variable at the output, ψ' is the state variable at the input, and T_q are the rearward transmission matrices. The response of the payload as a function of the input to the orbiter is thus obtained from Eqs. (7) and (10) as

$$\begin{Bmatrix} F_2 \\ A_2 \end{Bmatrix}=\begin{bmatrix} J_2 & B_2 \\ C_2 & D_2 \end{bmatrix}\begin{bmatrix} J_1 & B_1 \\ C_1 & D_1 \end{bmatrix}\begin{Bmatrix} F_1' \\ A_1' \end{Bmatrix} \tag{12}$$

where the output of the orbiter

$$\begin{Bmatrix} F_1 \\ A_1 \end{Bmatrix}$$

from Eq. (10) has been substituted for the input to the payload

$$\begin{Bmatrix} F_2' \\ A_2' \end{Bmatrix}$$

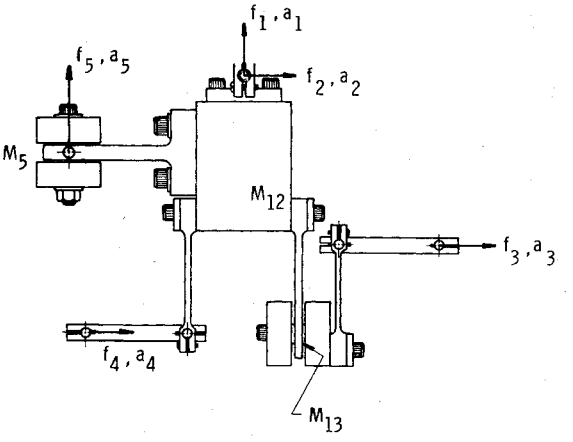

Fig. 2 Flexible payload model showing measurement coordinate system.

in Eq. (7). Note that F_1 has been equated to F_2' and not to $-F_2'$. While it is true that the $\Sigma F=0$ at the junction, the formulation of the transmission matrices is such that the output *by* the terminals of the orbiter, F_1, is positive, as is the input *to* the terminals on the payload, F_2'.

Application to Specific Model

For the present study, consider the payload and orbiter configurations shown in Figs. 2 and 3, respectively. The payload will have attach or input points 1-4, and one output point 5. The output will be free so that $F_5=0$. For this case we can write Eq. (1) more explicitly as

$$\left\{\begin{array}{c} a_5 \\ \hline a_1 \\ a_2 \\ a_3 \\ a_4 \end{array}\right\} = \left[\begin{array}{c|cccc} b_{55} & b_{51} & b_{52} & b_{53} & b_{54} \\ \hline b_{15} & b_{11} & b_{12} & b_{13} & b_{14} \\ b_{25} & b_{21} & b_{22} & b_{23} & b_{24} \\ b_{35} & b_{31} & b_{32} & b_{33} & b_{34} \\ b_{45} & b_{41} & b_{42} & b_{43} & b_{44} \end{array}\right] \left\{\begin{array}{c} -f_5 \\ \hline f_1 \\ f_2 \\ f_3 \\ f_4 \end{array}\right\} \tag{13}$$

where the acceleration and force components correspond to the coordinate system given in Fig. 2. Note that the dashed lines partition the admittance matrix into the form corresponding to that in Eq. (1).

Similarly for the orbiter, corresponding to Eq. (9) and Fig. 3, one can write

$$\left\{\begin{array}{c} a_1 \\ a_2 \\ a_3 \\ a_4 \\ \hline a_6 \\ a_7 \\ a_8 \\ a_9 \end{array}\right\} = \left[\begin{array}{cccc:cccc} c_{11} & c_{12} & c_{13} & c_{14} & c_{16} & c_{17} & c_{18} & c_{19} \\ c_{21} & c_{22} & c_{23} & c_{24} & c_{26} & c_{27} & c_{28} & c_{29} \\ c_{31} & c_{32} & c_{33} & c_{34} & c_{36} & c_{37} & c_{38} & c_{39} \\ c_{41} & c_{42} & c_{43} & c_{44} & c_{46} & c_{47} & c_{48} & c_{49} \\ \hdashline c_{61} & c_{62} & c_{63} & c_{64} & c_{66} & c_{67} & c_{68} & c_{69} \\ c_{71} & c_{72} & c_{73} & c_{74} & c_{76} & c_{77} & c_{78} & c_{79} \\ c_{81} & c_{82} & c_{83} & c_{84} & c_{86} & c_{87} & c_{88} & c_{89} \\ c_{91} & c_{92} & c_{93} & c_{94} & c_{96} & c_{97} & c_{98} & c_{99} \end{array}\right] \left\{\begin{array}{c} -f_1 \\ -f_2 \\ -f_3 \\ -f_4 \\ \hline f_6 \\ f_7 \\ f_8 \\ f_9 \end{array}\right\} \tag{14}$$

Note that point 5 does not appear on the orbiter. Again, the dashed lines indicate a partition corresponding to Eq. (9).

The procedure for the application of the transmission matrices now becomes clear. The elements of the admittance matrices in Eqs. (13) and (14) must be measured by experiments on the payload and orbiter individually. Substitution of the values into these matrices then allows subsequent matrix manipulations according to the previously outlined development. Ultimately, Eq. (12) is then used to predict the response of point 5 on the payload to an arbitrary input at points 6, 7, 8, and 9 of the orbiter.

Admittance Matrix Formulation

During the process of applying the above method to the prediction problem, it was discovered that another, simpler technique could be applied. As a result, both methods were studied and the results compared. The second method will be referred to as the admittance matrix method, and will now be described. One development for this method is given in Ref. 4. However, here the prediction equation will be derived directly from Eq. (12). This development will be applicable only for a case where the payload output force is zero in the coupled system (as is the present case).

In this equation, multiply the left hand side by

$$(H_2+E_1)^{-1}(g_{2\ell}^T g_{2\ell})^{-1} g_{2\ell}^T$$

Consider $F_2=0$ in Eq. (12) and perform the indicated matrix multiplications

$$0=(J_2J_1+B_2C_1)F_1'+(J_2B_1+B_2D_1)A_1' \tag{15a}$$

$$A_2=(C_2J_1+D_2C_1)F_1'+(C_2B_1+D_2D_1)A_1' \tag{15b}$$

Now substitute Eqs. (8) and (11) into Eq. (15a) to obtain

$$[g_{2\ell}(H_2+E_1)g_{1\ell}H_1-g_{2\ell}G_1^T]F_1' = g_{2\ell}(H_2+E_1)g_{1\ell}A_1'$$

There results

$$g_{1\ell}A_1'=[g_{1\ell}H_1-(H_2+E_1)^{-1}G_1^T]F_1' \tag{16}$$

Now substitute Eqs. (8) and (11) into Eq. (15b) to obtain

$$A_2=[-E_2g_{2\ell}(H_2+E_1)g_{1\ell}H_1+G_2^Tg_{1\ell}H_1 + E_2g_{2\ell}G_1^T]F_1'+[E_2g_{2\ell}(H_2+E_1)-G_2^T]g_{1\ell}A_1'$$

Into this, substitute Eq. (16), perform the matrix multiplication, and clear to obtain

$$A_2=G_2^T(H_2+E_1)^{-1}G_1^TF_1'$$

Since $A_2=a_5$ for the present case this becomes

$$a_5=G_2^T(H_2+E_1)^{-1}G_1^TF_1' \tag{17}$$

Description of Apparatus and Procedures

A description of the physical models, their associated instrumentation, and data acquisition procedures will be given in this section.

Orbiter

A schematic of the experimental orbiter model is shown in Fig. 3. The orbiter is symmetrical relative to a central plane

parallel to the paper in Fig. 3. The model is 69.3 cm (27.25 in.) long and consists of two identical 22.9 cm (9 in.) long cylindrical tanks separated by a center payload section. Each cylindrical tank was rolled from 0.305 mm (0.012 in.) thick 1100-H14 aluminum sheets to an outer diameter of 15.24 cm (6 in.) and butt-welded along the longitudinal seam. Flanges were spot-welded to both ends of each tank, allowing the tanks to be bolted to heavy end plates. The steel end plates were designed to reduce frequencies of the overall bending, torsion, and longitudinal modes into a useful range for making admittance measurements. The center payload section consists of an aluminum payload support ring which is bonded to two plastic bars that form a bending backbone for the model. These bars were made of polyvinyl chloride to provide bending mode damping from 1% to 2% critical. One vertical and three horizontal-acting mounting points were provided for the payload. These mountings were commercially-available flexure pivots so that they behaved as pure pin joints, whereby no moment could be transmitted through them. An additional mass (M_{10}) was supported on a plastic cantilever beam to represent an arbitrary additional elastic degree of freedom of some internal component.

Payload

The payload, shown in Fig. 2, consists of three masses, M_{12}, M_{13}, and M_5, joined by plastic beams and supported by aluminum links attached to the aluminum ring of the center section. Both masses M_{12} and M_{13} are made of steel, while mass M_5 is made of lead. Flexural pivot pins were used at attach points 1, 2, 3, and 4 to insure that loads perpendicular to one of the attach points would be transmitted faithfully without any moment being produced, as mentioned previously. For a blocked impedance test, a minor redesign to the attachment for points 1 and 2 was necessary. A double pin or yoke attachment was used at the joint so that the 1-direction was fixed independently of the 2-direction. More details on the models and test procedures can be obtained from Ref. 5.

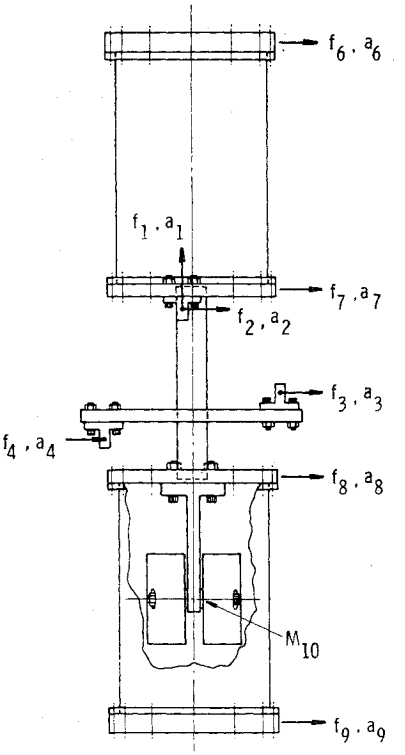

Fig. 3 Orbiter model showing measurement coordinate system.

Table 1 Test sequence for system with payload[a]

I. General

Steady-state sinusoidal acceleration responses are obtained for a single fixed amplitude forced response as outlined below. Data are taken at each of the following frequencies:

5.0,	10.0,	10.9,[b]	12.0,	15.0,	16.8,[c]
19.0,	20.3,[b]	21.5,[b]	23.0,	24.3,[b]	27.0,
29.0,	31.0,[b]	32.0,	37.0,	45.0,	47.6,[b]
50.0,	60.0	−Hz.			

II. Combined system

Excite at f_8, read accelerations a_5, a_6, a_7, a_8, a_9.

III. Payload

A) Excite at f_1, read accelerations a_1, a_2, a_3, a_4, a_5.
B) Excite at f_2, read same accelerations.
C) Excite at f_3, " " "
D) Excite at f_4, " " "
E) Excite at f_5, " " "

IV. Orbiter

A) Excite at f_1, read accelerations a_1, a_2, a_3, a_4, a_6, a_7, a_8, a_9.
B) Excite at f_2, read same accelerations.
C) Excite at f_3, " " "
D) Excite at f_4, " " "
E) Excite at f_6, " " "
F) Excite at f_7, " " "
G) Excite at f_8, " " "
H) Excite at f_9, " " "

[a] Coordinate system for these parameters defined in Figs. 2 and 3.
[b] Resonance frequencies for combined system.
[c] Anti-resonance frequencies for combined system.

Admittance Tests

The admittance tests consisted of acquiring steady-state sinusoidal response data from which mechanical admittance values could be computed for a given component or system. The item was suspended in a low frequency support in order to simulate a free-free configuration. Small piezoelectric accelerometers were used to measure responses at the designated points, while a constant force excitation signal was applied by a light electromagnetic coil. A similar arrangement was used for the flexible payload.

Initially, sine sweeps of constant force amplitude applied at one point were conducted and responses at selected points were recorded on an X-Y plotter. In order to obtain a good signal-to-noise ratio, both input and output were filtered through tracking filters having two-hertz band-widths. The signal was subsequently passed through a log converter in order to allow plotting of signals having a wide dynamic range. After initial tests, admittance data were taken at certain selected discrete frequencies. Both real and imaginary (CO and QUAD) values of admittance were read after being computed by a CO/QUAD analyzer. The data were read visually from a digital voltmeter, and later key-punched into input format for a digital computer. Overall accuracy available with this system was estimated at 5% to 10% maximum error.

A typical test sequence for the combined system, payload, and orbiter is given in Table 1. Initially, the combined system with payload installed was tested in order to obtain optimum frequencies at which subsequent data would be acquired. (This procedure was followed in order to reduce the number of measurements required for this study and would not normally be applied in practice.) Since all parameters were frequency-dependent, it is obvious that subsequent measurements performed for different setup positions had to be made at exactly the same frequencies. Thus, the twenty discrete frequencies indicated were chosen as a good represen-

tation of resonance, anti-resonance, and between-resonance frequencies. It was also decided that the results of Step II for the combined system (i.e., a_5/f_8, with $f_6, f_7, f_9 = 0$) would be chosen as the response with which to compare subsequent predicted values.

Steps III and IV in Table 1 describe the sequence used for acquiring the admittance data for these components. Note that each case required a different setup for the excitation coil, and data had to be acquired for each of the twenty frequencies for each setup. Obviously, a large volume of data was necessary for the indicated procedure which was applicable to the transmission matrix method. Significantly fewer measurements were necessary for application of the admittance matrix method, as can be seen from a careful study of the dimension of the matrices derived for that method.

Blocked Impedance Tests

A blocked impedance test also was performed on the flexible payload. It was felt that responses for this condition may be more like those on the payload installed in the orbiter, and increased prediction accuracy might therefore result. Some modification of the connecting links was necessary in order to attach the payload at points 1 and 2 independently. That is, the payload was attached in the 1-direction independently of the 2-direction. This was accomplished by use of a double pin at the joint. Also, the payload was mounted to a massive rigid fixture through very stiff piezoelectric force transducers which did not allow motion at the blocked points. One attachment point was left free and the small exciter along with an accelerometer were attached.

For these tests, the input acceleration was maintained constant and the resultant forces at the input and the three other response points were recorded. Measurements were made at each of the discrete frequencies previously used for the admittance tests. As in the admittance tests, the force signals

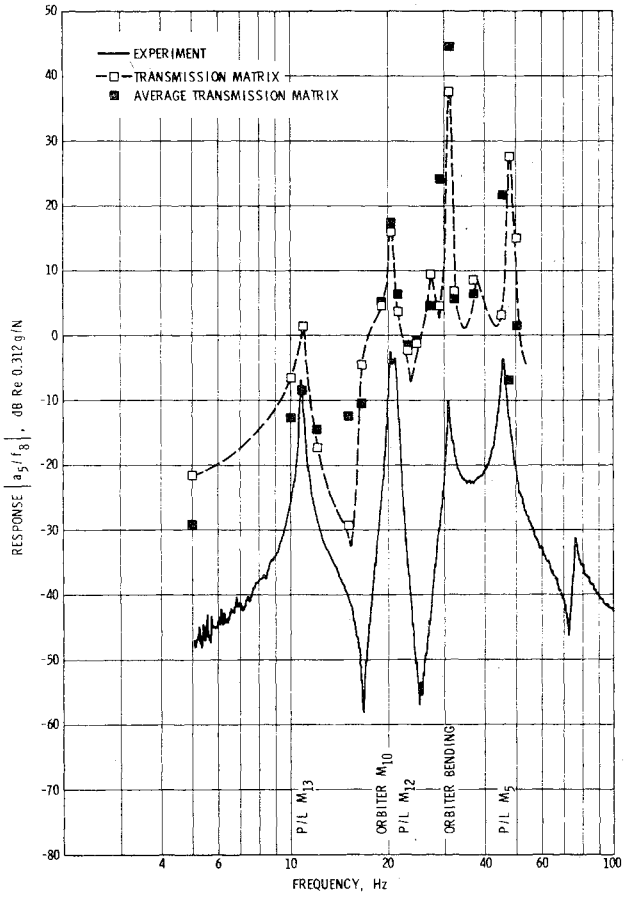

Fig. 4 System response with payload installed—transmission matrix method.

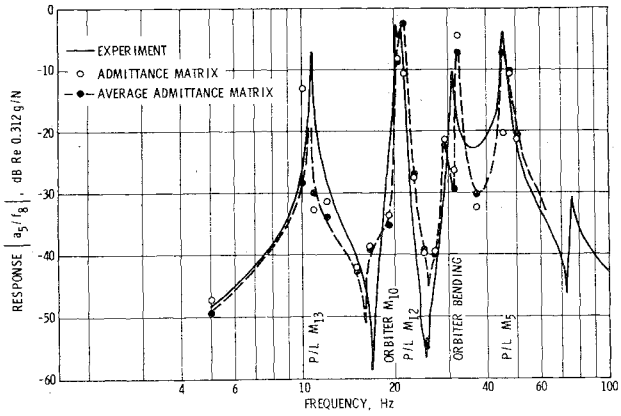

Fig. 5 System response with payload installed—admittance matrix method.

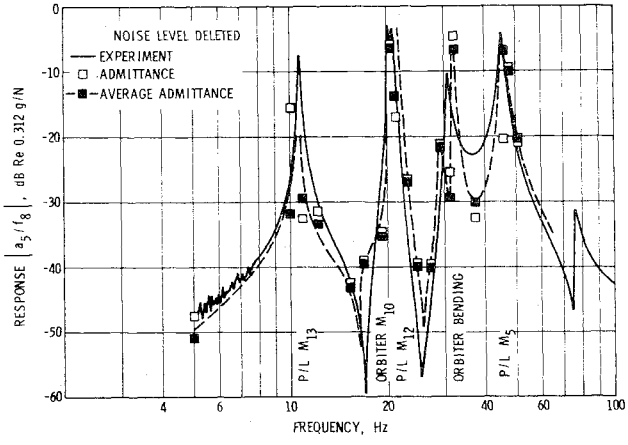

Fig. 6 Influence of matrix error on system response.

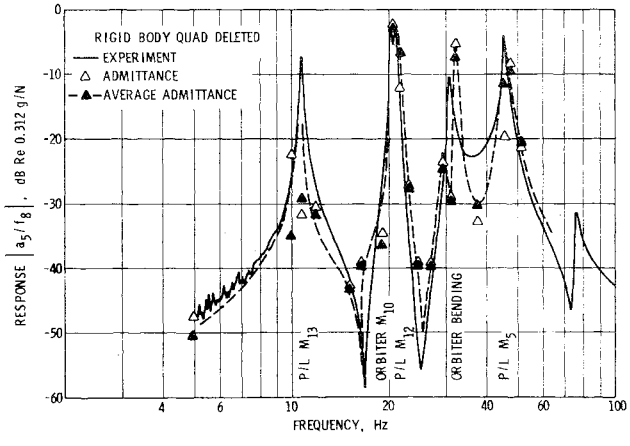

Fig. 7 Influence of rigid body error on system response.

and the constant acceleration were filtered, then input to the CO/QUAD analyzer to compute real and imaginary parts of the complex inpedances.

Analytical and Experimental Results

Transmission Matrix Method

Numerical values for the complex admittances read at each of the discrete frequencies listed in Table 1 will not be tabulated for the sake of brevity. Rather, final results will be given in terms of a comparison of measured and predicted values on similar frequency response plots.

Results for the transmission matrix method are shown in Fig. 4. Computed predictions, which are based on the use of Eq. (12), were finally obtained at nineteen different frequen-

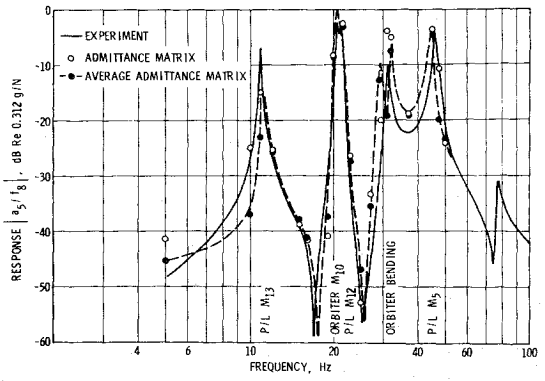

Fig. 8 System response with payload—blocked impedance results.

cies identified in Table 1 (60 Hz was omitted because of electrical noise problems). The predicted points identified as "transmission matrix" were obtained from use of "as measured" admittances, which resulted in some nonsymmetry in the admittance matrices. This was considered to be measurement error, and a second set of results, identified as "average transmission matrix" was computed by averaging the corresponding off-diagonal matrix elements and using the resulting symmetrical matrices in the computations. In either case, however, it is obvious that the correspondence between predicted and measured response is very poor, although the qualitative shape of the curve is apparent. Repeated attempts were conducted to determine whether the wide discrepancy was caused by programming error. No such error was discovered. The final conclusion reached was that the error is genuinely inherent in the use of the transmission matrix method, although the fact that essentially all results were too large did seem peculiar.

Admittance Matrix Method

Typical final results using this method for the system with payload installed are given in Fig. 5. Computed values are based on the use of Eq. (17). It is apparent that a reasonably acceptable comparison is achieved for this method, and for most of the data, "as measured" or "averaged" results are essentially the same. However, significant differences appear to result from matrix nonsymmetry near resonance values. In some cases the nonsymmetry was as much as 100%. These errors obviously reflect the extreme sensitivity of the results near resonance to small differences in test conditions. The dashed lines are drawn to show an extrapolation between the average admittance values. It appears that this method produces the best overall results.

Some results of attempts at error analysis are given in Figs. 6 and 7. It was recognized that some noise level was present in the measured data. This was arbitrarily taken as 0.01 of the largest admittance value present at a given frequency. All matrix elements below this value were set equal to zero in both the payload and orbiter matrices, and final results again computed. From Fig. 6 it appears that this procedure caused no significant difference in the final results.

A second attempt at error analysis was conducted by deleting the QUAD (or imaginary) value of admittance that occurred at 5 Hz. It is recognized that at this frequency the motion of both components is essentially that of a rigid body, and the admittances should be purely real numbers. The 5-Hz value of QUAD as measured was considered error, and was deleted from all other values measured at other frequencies. The resulting matrices were again used for prediction through Eq. (17). Again, however, significant differences in the results were not apparent, as can be seen by comparing Figs. 5 and 7.

Admittance/Impedance Matrix Method

Although Eq. (17) has been derived in terms of admittance parameters, it can also be used for the case of blocked impedance measurements on the payload. In this case, the impedance test results are formed into a 4×4 impedance matrix Z_2 for the payload while it was tested alone. Then note that

$$H_2 = Z_2^{-1} \tag{18}$$

This expression was combined with Eq. (17) to form another prediction method which uses admittance measurements on the orbiter, and impedance measurement on the payload.

Final results based on the above method are shown in Fig. 8. Comparison of these results with those in Fig. 6 reveal that there is no significant difference in the results of the admittance/impedance method.

Conclusions

In view of the preceding results and implications, several positive conclusions can be identified from this study.

1) The transmission matrix method is undesirable for prediction of payload responses in the combined system if measured component parameters are to be utilized.

2) The admittance matrix method produces a satisfactory prediction of payload responses under similar input conditions. It also requires fewer measurements than the transmission matrix method.

3) Use of forced symmetry by averaging off-diagonal admittance elements is desirable.

4) Noise error of the order of 0.01 of the maximum measured values at a given frequency has no effect on the final results.

5) Simulated free-free admittance or fixed boundary blocked impedance tests for the payload appear to produce similar accuracy in prediction.

6) Use of steady-state sinusoidal procedures for data acquisition is extremely cumbersome and time-consuming. For practical application of these techniques a far more rapid and automated data acquisition process will be required.

7) The reader must interpret these results with caution. Note especially that momentless connections were used at the interface. Use of more general connections would require further validation before the method is applied to such a case.

References

[1] Klosterman, A.L., and Lemon, J.R., "Dynamic Design Analysis via the Building Block Approach," *Shock and Vibration Bulletin* No. 42, Pt. 1, pp. 97-104.

[2] Flannelly, W.G., Berman, A., and Barnsby, W.G., "Theory of Structural Dynamic Testing Using Impedance Techniques," Vol. I, Theoretical Development, USAAVLABS Technical Report 70-6A, June 1970.

[3] Rubin, S., "Transmission Matrices for Vibration and Their Relation to Admittance and Impedance," *ASME Transactions, Series B, Journal of Engineering for Industry*, Vol. 86, 1964, pp. 9-21.

[4] Noiseux, D.E., and Meyer, E.B., "Application of Impedance Theory and Measurements to Structural Vibration," AFFDL-TR-67-182, Aug. 1968, Air Force Flight Dynamics Lab., Wright-Patterson AFB, Ohio.

[5] Kana, D.D., and Vargas, L.M., "Prediction of Payload Vibration Environments by Mechanical Admittance Test Techniques," NASA CR-2591, 1975.